

This is an Open Access document downloaded from ORCA, Cardiff University's institutional repository: <https://orca.cardiff.ac.uk/id/eprint/97963/>

This is the author's version of a work that was submitted to / accepted for publication.

Citation for final published version:

Burnley-Hall, Nicholas, Willis, Gareth, Davis, Jessica, Rees, Dafydd Aled and James, Philip E 2017. Nitrite-derived nitric oxide reduces hypoxia-inducible factor 1 $\alpha$ -mediated extracellular vesicle production by endothelial cells. *Nitric Oxide: Biology and Chemistry* 63 , pp. 1-12. 10.1016/j.niox.2016.12.005

Publishers page: <http://dx.doi.org/10.1016/j.niox.2016.12.005>

Please note:

Changes made as a result of publishing processes such as copy-editing, formatting and page numbers may not be reflected in this version. For the definitive version of this publication, please refer to the published source. You are advised to consult the publisher's version if you wish to cite this paper.

This version is being made available in accordance with publisher policies. See <http://orca.cf.ac.uk/policies.html> for usage policies. Copyright and moral rights for publications made available in ORCA are retained by the copyright holders.



1 **Nitrite-derived nitric oxide reduces hypoxia-inducible factor 1 $\alpha$ -**  
2 **mediated extracellular vesicle production by endothelial cells**

3 *Nicholas Burnley-Hall<sup>1\*</sup>, Gareth Willis<sup>2\*</sup>, Jessica Davis<sup>3</sup>, D. Aled Rees<sup>4</sup>, Philip E. James<sup>5</sup>.*

4 <sup>1</sup>School of Medicine, Cardiff University, Cardiff, CF24 4HQ

5 <sup>2</sup>Division Newborn Medicine, Boston Children's Hospital, Harvard Medical School, Harvard  
6 University, Boston, USA, MA 02115.

7 <sup>3</sup>Institute of Cancer & Genetics, Cardiff University, Cardiff, UK, CF14 4XN

8 <sup>4</sup>Neurosciences and Mental Health Research Institute, School of Medicine, Cardiff University,  
9 Cardiff, UK, CF24 4HQ

10 <sup>5</sup>Cardiff School of Health Sciences, Cardiff Metropolitan University, Cardiff, CF5 2SG

11 \*Authors contributed equally to this work.

12 **Running title:** Nitric oxide reduces vesicle production in hypoxia.

13 Correspondence address and request for reprints to: Professor Philip James

14 Cardiff School of Health Sciences, Cardiff Metropolitan University, Cardiff, CF5 2YB

15 Email: [PJames@cardiffmet.ac.uk](mailto:PJames@cardiffmet.ac.uk) Telephone: +44 02920 417129

16

17

18

19

20

21

22

23 **Highlights**

- 24 • Hypoxia-inducible factor 1 $\alpha$ , but not 2 $\alpha$ , mediates extracellular vesicle release in  
25 endothelial cells
- 26 • Nitrite-derived nitric oxide increases HIF-1 $\alpha$  degradation, and subsequently  
27 reduces extracellular vesicle production
- 28 • This effect is attenuated by inhibition of xanthine oxidoreductase, preventing the  
29 conversion of nitrite to nitric oxide.

30 **Summary**

31 **Introduction:** Extracellular vesicles (EVs) are small, spherical particles enclosed by a phospholipid  
32 bilayer (~30-1000nm) released from multiple cell types, and have been shown to have  
33 pathophysiological roles in a plethora of disease states. The transcription factor hypoxia-inducible  
34 factor-1 (HIF-1) allows for adaptation of cellular physiology in hypoxia and may permit the enhanced  
35 release of EVs under such conditions. Nitric oxide (NO) plays a pivotal role in vascular homeostasis,  
36 and can modulate the cellular response to hypoxia by preventing HIF-1 accumulation. We aimed to  
37 selectively target HIF-1 via sodium nitrite (NaNO<sub>2</sub>) addition, and examine the effect on endothelial  
38 EV, size, concentration and function, and delineate the role of HIF-1 in EV biogenesis.

39 **Methods:** Endothelial (HECV) cells were exposed to hypoxic conditions (1% O<sub>2</sub>, 24 hours) and  
40 compared to endothelial cells exposed to normoxia (21% O<sub>2</sub>) with and without the presence of sodium  
41 nitrite (NaNO<sub>2</sub>) (30 μM). Allopurinol (100 μM), an inhibitor of xanthine oxidoreductase, was added  
42 both alone and in combination with NaNO<sub>2</sub> to cells exposed to hypoxia. EV and cell preparations  
43 were quantified by nanoparticle tracking analysis and confirmed by electron microscopy. Western  
44 blotting and siRNA were used to confirm the role of HIF-1α and HIF-2α in EV biogenesis. Flow  
45 cytometry and time-resolved fluorescence were used to assess the surface and intravesicular protein  
46 content.

47 **Results:** Endothelial (HECV) cells exposed to hypoxia (1% O<sub>2</sub>) produced higher levels of EVs  
48 compared to cells exposed to normoxia. This increase was confirmed using the hypoxia-mimetic  
49 agent desferrioxamine. Treatment of cells with sodium nitrite (NaNO<sub>2</sub>) reduced the hypoxic  
50 enhancement of EV production. Treatment of cells with the xanthine oxidoreductase inhibitor  
51 allopurinol, in addition to NaNO<sub>2</sub> attenuated the NaNO<sub>2</sub>-attributed suppression of hypoxia-mediated  
52 EV release. Transfection of cells with HIF-1α siRNA, but not HIF-2α siRNA, prior to hypoxic  
53 exposure prevented the enhancement of EV release.

54 **Conclusion:** These data provide evidence that hypoxia enhances the release of EVs in endothelial  
55 cells, and that this is mediated by HIF-1α, but not HIF-2α. Furthermore, the reduction of NO<sub>2</sub><sup>-</sup> to NO  
56 via xanthine oxidoreductase during hypoxia appears to inhibit HIF-1α-mediated EV production.

57 **Key words:** Extracellular vesicles, hypoxia, hypoxia-inducible factor, nitrite, nitric oxide

58

59 **Abbreviations**

- 60 Extracellular vesicles (EVs)
- 61 Hypoxia-inducible factor 1 (HIF-1)
- 62 Nitrate ( $\text{NO}_3^-$ )
- 63 Nitrite ( $\text{NO}_2^-$ )
- 64 Nitric oxide (NO)
- 65 Nanoparticle tracking analysis (NTA)
- 66 Sodium nitrite ( $\text{NaNO}_2$ )
- 67 Time-resolved fluorescence (TRF)

## 68 1. Introduction

69 The production of extracellular vesicles (EVs) is a common feature of eukaryotic cells, including  
70 platelets, leukocytes, and endothelial cells [1]. EVs are spherical, submicron structures enclosed by a  
71 phospholipid bilayer, containing a variety of proteins, mRNAs and microRNAs [2]. Their application  
72 to modulate physiology is complex, with evidence for them both augmenting and alleviating disease,  
73 depending on their cellular origin and subsequent biophysical composition [3]. Elevated levels of EVs  
74 have been shown to have pathophysiological roles in a plethora of disease states, including cancer [4–  
75 6], neurodegenerative disorders [7–10], and cardiovascular disease [11–13]. Specifically, endothelial  
76 cell derived EVs have been shown to express tissue factor, suggesting a role in augmenting the  
77 coagulation cascade [14]. Additionally, EVs from patients with myocardial infarction have been  
78 shown to induce endothelial dysfunction *ex vivo* [15]. It has recently been shown that endothelial  
79 cells enhance EV secretion following temporary hypoxia exposure *in vivo* [16,17], a fundamental  
80 feature of the aforementioned diseases and resulting pathologies [18–20]. Indeed, EVs derived from  
81 endothelial cells exposed to hypoxia have been shown to produce a markedly altered RNA and protein  
82 composition, although the function of these EVs remains undetermined [21].

83 The adaptation of cellular physiology in response to hypoxia is largely mediated by the transcription  
84 factor hypoxia-inducible factor (HIF)-1, which promotes the transcription of genes involved in cell  
85 proliferation, metastasis, angiogenesis, and vascular remodelling [22,23]. HIF is comprised of an  
86 oxygen regulated HIF- $\alpha$  subunit (HIF-1 $\alpha$  or HIF-2 $\alpha$ ) and the constitutively expressed HIF-1 $\beta$ . Whilst  
87 HIF-1 $\alpha$  is ubiquitously expressed, HIF-2 $\alpha$  is detected predominantly in vascular endothelial cells [24].  
88 The HIF- $\alpha$  subunit is targeted for degradation under normoxic conditions by the O<sub>2</sub>-dependent HIF- $\alpha$   
89 prolyl hydroxylase enzymes. These enzymes hydroxylate two conserved prolyl residues (Pro 564 and  
90 Pro402) in the central oxygen-dependent degradation domain of the HIF- $\alpha$  subunit (both HIF-1 $\alpha$  and  
91 HIF-2 $\alpha$ ), which promotes the binding of the Von Hippel-Lindau protein, allowing ubiquitination and  
92 subsequent degradation [25,26]. Inhibition of these enzymes in hypoxia prevents the degradation of  
93 HIF- $\alpha$ , allowing regulation of its transcriptional target genes [25]. HIF has been shown to increase  
94 expression of several proteins involved in cytoskeletal changes [27], a mechanism thought to be  
95 implicated in augmented EV release [28]. Thus, selective targeting and modulation of HIF- $\alpha$  could  
96 modulate endothelial cell EV release.

97 Endothelial-derived nitric oxide (NO) plays a pivotal role in vascular homeostasis, highlighted by the  
98 deficiency of NO prevalent in cardiovascular disease states [29]. NO can modulate the cellular  
99 response to hypoxia by preventing the stabilization of HIF- $\alpha$  via an increase in prolyl hydroxylase-  
100 mediated degradation [30,31]. Previously, impaired endogenous NO production in HUVECs has been  
101 shown to increase EV formation [32]. Recently, the inorganic anions nitrate (NO<sub>3</sub><sup>-</sup>) and nitrite (NO<sub>2</sub><sup>-</sup>),

102 once thought to be inert end products of NO metabolism, have been shown to be bioactive reservoirs  
103 for NO bioactivity, particularly during hypoxia [33,34].  $\text{NO}_3^-$  is reduced to  $\text{NO}_2^-$  via commensal  
104 bacteria present in the oral cavity.  $\text{NO}_2^-$  can subsequently be reduced through reaction with various  
105 proteins that possess  $\text{NO}_2^-$  reductase activity, including Xanthine Oxidoreductase (XOR) [35,36],  
106 heme globins [37,38], and components of the mitochondrial electron transport chain [39,40].

107 Here, we aimed to elucidate the role of both HIF-1 $\alpha$  and HIF-2 $\alpha$  in endothelial EV release, and  
108 selectively target their expression in hypoxia via sodium nitrite ( $\text{NaNO}_2$ ) addition, and investigate the  
109 effect on endothelial cell EV production.

## 110 **2. Methods**

### 111 **2.1 Cell culture & viability**

112 Human (HECV) endothelial cells were purchased from Interlab Cell Line Collection (ICLC, Naples,  
113 Italy). This cell line was used as a convenient model of endothelial cell behaviour. HECVs were  
114 maintained in Dulbecco's Modified Eagle Medium (DMEM, PAA Laboratories Ltd, UK)  
115 supplemented with 10% foetal calf serum (FCS, PAA Laboratories Ltd, UK), and 1%  
116 penicillin/streptomycin (P/S, Gibco®, Life Technologies, UK). Human umbilical vein endothelial  
117 cells (HUVECs) were isolated from umbilical cords as previously described [41]. Human umbilical  
118 cords were obtained from the Antenatal Clinic, University Hospital Wales. Ethical approval was  
119 obtained from the Research Ethics Committee (REC) (REC reference: 14/NW/1459). HUVECs were  
120 maintained in M199 medium, supplemented with 10% foetal calf serum, 1% penicillin/streptomycin,  
121 human epidermal growth factor (1 ng/mL, Invitrogen, UK) and hydrocortisone (1 ng/mL, Sigma-  
122 Aldrich, UK). HUVECs were used at passage 0 and not sub-cultured. Cells were cultured using T25  
123 cm<sup>2</sup> flasks (Cellstar®, Greiner Bio-One, Germany) and maintained in an incubator at 37 °C and 5%  
124 CO<sub>2</sub>. Cell counts were undertaken using trypan blue exclusion (1:1 v/v) and a Cellometer Auto T4  
125 (Nexcelom Biosciences, USA). Cell viability and apoptosis were determined using MTS and Caspase-  
126 Glo 3/7 assays (Promega, Southampton, UK), respectively, according to the manufacturers'  
127 instructions.

### 128 **2.2 Hypoxia exposure**

129 Hypoxic experiments were performed using an I-CO<sub>2</sub>N<sub>2</sub> regulated InVivo 400 hypoxia workstation  
130 (Ruskin, Bridgend, UK). Upon cells reaching ~80% confluency, culture medium was removed.  
131 HECVs were washed with phosphate-buffered saline (PBS) (Fisher Scientific, UK) and incubated  
132 with 10 mL EV-free serum free medium (SFM) for 24-hours. Cells were cultured at either normoxia  
133 (21% O<sub>2</sub>, 5% CO<sub>2</sub>, 37 °C) or hypoxia (1-20% O<sub>2</sub>, 5% CO<sub>2</sub>, 37 °C). The hypoxia mimetic agent  
134 desferrioxamine was added (100 μM) to HECVs incubated in normoxia to confirm the role of hypoxia  
135 in EV formation.

### 136 **2.3 Extracellular vesicle isolation**

137 EVs were isolated direct from cell culture as previously described [42]. Cells were cultured in serum-  
138 free medium (SFM) for 24 hours prior to EV isolation to avoid contamination from foetal calf serum.  
139 Cell culture medium was extracted direct from the culture flask and subjected to differential ultra-  
140 centrifugation. Culture medium was spun at 500 × g for 10 min to remove any cells in suspension.  
141 The supernatant was then centrifuged at 15,000 × g for 15 min to remove any cell debris. Finally,



142 supernatants were ultracentrifuged at  $100,000 \times g$  for 60 min to pellet EVs. This pellet was then  
143 resuspended in 1 x sterile PBS, stored at  $4^{\circ}\text{C}$  and analysed within 1 week of isolation.

#### 144 **2.4 EV size and concentration analysis**

145 Size and concentration distributions of EVs were determined using nanoparticle tracking analysis  
146 (NTA, NanoSight LM10 system, UK) as described previously [43]. NTA is a laser illuminated  
147 microscopic technique equipped with a 642 nm laser and a high sensitivity digital camera system  
148 (OrcaFlash2.8, Hamamatsu, NanoSight Ltd) that determines the Brownian motion of nanoparticles in  
149 real-time to assess size and concentration. Sixty-second videos were recorded and particle movement  
150 was analysed using NTA software (version 2.3). Camera shutter speed was fixed at 30.01 ms and  
151 camera gain to 500. Camera sensitivity and detection threshold were (11–14) and (4–6), respectively.  
152 A representative NTA trace can be seen in Appendix Figure A1. EV samples were diluted in EV-free  
153 sterile water (Fresenius Kabi, Runcorn, UK). Samples were run in quintuplicate, from which EV  
154 distribution, size and average concentration were calculated. EV concentrations were then normalised  
155 to cell count and expressed as EVs/cell.

#### 156 **2.5 Silencing RNA (siRNA) transfection**

157 siRNA specific for HIF-1 $\alpha$  (Dharmacon SMARTpool, UK) was mixed with siRNA transfection  
158 reagent (Dharmacon RNAi Technologies) at a ratio of 20:1 and incubated at room temperature for 20  
159 minutes. This mix was added to the medium of ~50% confluent HECV cells to give a final  
160 concentration of 100 nM per flask. Control experiments consisted of transfection with the ON-  
161 TARGETplus non-targeting siRNA control (100 nM; Dharmacon RNAi Technologies). Cells were  
162 incubated in medium containing either HIF-1 $\alpha$  siRNA or control siRNA for 48-72 hours prior to  
163 hypoxia exposure for 24 hours.

164 For HIF-2 $\alpha$  silencing, the siRNA duplex was mixed with siRNA transfection reagent (Santa Cruz  
165 Biotechnology, USA) (1:1 ratio) in transfection medium and incubated at room temperature for 30  
166 minutes before being added onto the cells. Cells were incubated for 5 hours before 2x DMEM (20%  
167 FCS, 2% P/S) was added. Cells were incubated for an additional 24 hours before replacing the  
168 medium with fresh 1x DMEM (10% FCS, 1% P/S). Cells were incubated for an additional 48-72  
169 hours prior to hypoxia exposure for 24 hours.

#### 170 **2.6 Nitrite treatment and xanthine oxidoreductase inhibition**

171 Preliminary experiments established a  $\text{NaNO}_2$  dose-effect curve (0.3-300  $\mu\text{M}$ ) where 30 $\mu\text{M}$  was  
172 discovered to be the optimal dose and was used for all subsequent experiments (Appendix Figure A2).  
173 Cells were incubated in either hypoxia (1%  $\text{O}_2$ ), or normoxia for 24-hours. Allopurinol (100  $\mu\text{M}$ ) was  
174 added to inhibit the hypoxia mediated reduction of  $\text{NO}_2^-$  to NO by xanthine oxidoreductase in HECVs

175 exposed to hypoxia for 24 hours. The NO donor S-Nitrosoglutathione (GSNO, 10  $\mu$ M) was also  
176 added to cells to confirm the effect of NO on EV production.

## 177 **2.7 Western blot**

178 HECVs were washed with phosphate-buffered saline (PBS) and lysed in ice-cold Pierce® RIPA lysis  
179 buffer (ThermoFisher, UK). The lysates underwent centrifugation at 13,000 x g for 20 min at 4 °C.  
180 The supernatants were collected and their protein concentrations were determined by a Pierce® BCA  
181 Protein Assay Kit (ThermoFisher, UK), measured on a BMG CLARIOstar (BMG Labtech, UK). Cell  
182 homogenates (80  $\mu$ g protein) were separated by a 10% sodium dodecyl sulfate-polyacrylamide gel  
183 (SDS-PAGE) and transferred to a nitrocellulose membrane. After blots had been washed with TBST  
184 (10 mM Tris, 150 mM NaCl, 0.05% Tween-20; pH 7.6) the membrane was blocked with 5%  
185 skimmed milk powder in TBST for 1 hour and incubated overnight at 4 °C with a purified mouse  
186 monoclonal antibody against human HIF-1 $\alpha$  (BD Biosciences, UK), HIF-2 $\alpha$  (Santa Cruz, USA) or a  
187 rabbit monoclonal antibody against  $\beta$ -actin (Sigma-Aldrich, UK) at dilutions recommended by the  
188 manufacturers. The membranes were washed and then incubated for 1 hour with the required  
189 secondary IgG horseradish peroxidase labelled antibody (goat anti-mouse or goat anti-rabbit).  
190 Detection was performed using West Femto chemiluminescence detection reagent (Pierce and Warner  
191 Ltd, UK) and exposed to photographic film (Amersham™ Hyperfilm, GE Healthcare) in a dark room.  
192 Films were developed using Kodak™ -D19 developer and fixer (Sigma-Aldrich).

## 193 **2.8 Electron microscopy**

194 Scanning electron microscopy (EM) images were generated to confirm EV release under normoxic  
195 and hypoxic (1% O<sub>2</sub>) conditions. HECVs were washed in PBS and fixed in glutaraldehyde (Sigma-  
196 Aldrich, UK) in Sorensen's phosphate buffer (1% v/v) at room temperature for 1 hour. Samples were  
197 then dehydrated through graded isopropanol at 50, 70, 90 and 100% for 10 minutes each, followed by  
198 three exchanges in hexamethyldisilazane (Sigma-Aldrich, UK). Samples were then air dried and  
199 splutter-coated with gold and viewed at 5kV using a JEOL 840A scanning electron microscope (JEOL  
200 Tokyo, Japan).

201 Isolated EVs were visualised using transmission EM. Isolated EVs in PBS were negatively stained by  
202 placing carbon-coated grids onto 50  $\mu$ L droplet of reagent for 30 minutes. Vesicles were fixed in 1%  
203 glutaraldehyde in Sorensen's phosphate buffer (1:1 v/v) for 10 minutes at room temperature. Grids  
204 were then washed (3 x 1 min in PBS and 6 x 1 min in water) before negative staining with 2% (w/v)  
205 uranyl acetate for 10 min. Surplus staining was removed from grids and allowed to air dry before EV  
206 samples were examined in a Philips CM12 TEM (FEI UK Ltd) at 80 kV.

## 207 **2.9 Characterisation of EVs**

208 Flow cytometry was used to assess the surface adhesion molecule profile of HECVs incubated at both  
209 normoxia and hypoxia, and their corresponding EVs. Antibodies used for cytometric analysis were  
210 obtained from Biolegend® (BioLegend, San Diego, CA, USA). They include; anti-CD62P [P-  
211 selectin], anti-CD51P [VCAM-1], anti-CD54 [ICAM-1], anti-CD562E [E-selectin], anti-CD31  
212 [PECAM-1], and annexin V-FITC. Annexin V positivity was chosen to reflect the extent of  
213 phosphatidylserine (PS) exposure on the surface of EVs. All antibodies were allophycocyanin  
214 conjugated and mouse anti-human. Flow cytometry was performed using a BD Canto dual laser bench  
215 top flow cytometer, equipped with 488 nm and 633 nm lasers and BD FACS Diva software (v 5.0.3).  
216 Carboxylated polystyrene beads (200, 500 and 1000 nm in diameter, (IZON, Oxford, UK)) were used  
217 to set the EV gate, and were distinguishable as three distinct populations. HECVs were analysed for  
218 forward scatter area and side scatter area whilst EVs were run on forward scatter area and side scatter  
219 area that were set to logarithmic scale. Acquisition was terminated upon recording 10,000 events,  
220 gated based on their forward scatter and side scatter characteristics. Fluorescence minus one (FMO)  
221 stains were used to set the positive gates for each antibody. Appendix Figure A3 shows a  
222 representative dot plot showing fluorescence-minus-one (A) and the EV gating strategy (B).

223 Time-resolved fluorescence was used to assess the surface protein and content of the isolated EVs  
224 derived from both normoxia and hypoxia, as described previously [44].  $1 \times 10^9$  EVs were loaded onto a  
225 high protein binding 96-well plate (Greiner Bio-One, Germany) overnight at 4°C, before non-specific  
226 sites were blocked with 1% BSA (R&D Systems) for two hours. EVs were permeabilised using a  
227 RIPA lysis buffer (Santa Cruz, CA, USA) to allow analysis of intravesicular exosomal and endothelial  
228 markers. EVs were incubated overnight with mouse anti-human antibodies for the exosomal markers  
229 CD9, ALIX and TSG101, the endothelial marker CD144 (VE-Cadherin) and HIF-1 $\alpha$  (Abcam,  
230 Cambridge, UK) overnight at 4°C. Markers were detected using a biotinylated anti-mouse IgG  
231 secondary antibody (PerkinElmer, Buckinghamshire, UK) and a streptavidin:europium conjugate  
232 (PerkinElmer, Buckinghamshire, UK) and measured by time-resolved fluorescence (delay time: 400  
233  $\mu$ s, measurement window: 400  $\mu$ s) using a BMG Labtech FLUOstar Optima.

## 234 **2.10 Statistics**

235 Data were analysed using GraphPad Prism (version 5.0; GraphPad Software Inc., San Diego, USA).  
236 D'Agostino's K-squared test was used to check data for normality. A 2way ANOVA with Bonferroni  
237 correction was used to compare size distribution differences between hypoxia and normoxia. A 1way  
238 ANOVA followed by either a Dunnett's post-test to compare all groups to the normoxic control, or a  
239 Tukey's test to compare all pairs of columns with each other. Results are expressed as mean  $\pm$  SEM  
240 unless stated. A *p*-value of <0.05 was regarded as statistically significant.

241

242 **3. Results**

243 **3.1 Effect of hypoxia on EV size, concentration and distribution**

244 Hypoxia exposure (1%, 2% and 5% O<sub>2</sub>) enhanced EV production in comparison to HECVs  
245 maintained at normoxia (1% O<sub>2</sub>: 1766 ± 63.4 EVs/cell, 2% O<sub>2</sub>: 1179 ± 59 EVs/cell, 5% O<sub>2</sub>: 659 ± 48  
246 EVs/cell vs 21% O<sub>2</sub>: 133 ± 15 EVs/cell, Figure 1A, *p* < 0.001). However, 10% and 20% O<sub>2</sub> did not  
247 change EV production (10% O<sub>2</sub>: 190.2 ± 40 EVs/cell, 20% O<sub>2</sub>: 218 ± 57 EVs/cell *p*>0.05) compared  
248 to normoxia (Figure 1A). Hypoxic conditions did not affect EV mean size: 21% O<sub>2</sub>: 134 ± 8 nm; 1%  
249 O<sub>2</sub>: 131 ± 27 nm; 2% O<sub>2</sub>: 133 ± 33 nm; 5% O<sub>2</sub>: 143 ± 38 nm; 10% O<sub>2</sub>: 133 ± 38 nm, 20% O<sub>2</sub>: 132 ±  
250 30 nm, *p* > 0.05. Western blot analysis revealed the presence of HIF-1α in cells exposed to 1-5% O<sub>2</sub>  
251 for 24 hours. HIF-1α was not detected in cells exposed to 10% or 20% O<sub>2</sub> (Figure 1B).

252 On assessment of EV size distribution (split by 50 nm bin size for analysis), cells exposed to 1% O<sub>2</sub> in  
253 particular had an elevated EV concentration within a diameter range of 51 – 350 nm (51 – 100 nm:  
254 21% O<sub>2</sub>; 16 ± 5 EVs/cell vs 1% O<sub>2</sub>; 205 ± 44 EVs/ cell. 101 – 150 nm: 21% O<sub>2</sub>; 33 ± 8 EVs/cell vs  
255 1% O<sub>2</sub>; 441 ± 66 EVs/cell. 151 – 200 nm: 21% O<sub>2</sub>; 29 ± 5 EVs/cell vs 1% O<sub>2</sub>; 401 ± 26 EVs/ cell.  
256 201 – 250 nm: 21% O<sub>2</sub>; 22 ± 4 EVs/cell vs 1% O<sub>2</sub>; 300 ± 18 EVs/ cell. 251-300 nm: 21% O<sub>2</sub>; 14 ± 3  
257 EVs/cell vs 1% O<sub>2</sub>; 210 ± 30 EVs/ cell. 301-350 nm: 1% O<sub>2</sub>: 7 ± 2 EVs/cell vs 1% O<sub>2</sub>: 132 ± 22  
258 EVs/cell (*p* < 0.001 for all comparisons). EV distribution between 351 – 1 μm was similar between  
259 normoxic and hypoxic cells, *p* > 0.05 (Figure 2).

260 Cells incubated in normoxia exposed to the hypoxia mimetic agent desferrioxamine (100 μM)  
261 produced significantly higher EVs compared to cells exposed to normoxia alone (1212 ± 109 EVs/cell  
262 vs 133 ± 15.2 EVs/cell, *p* < 0.001). The addition of desferrioxamine to cells already exposed to  
263 hypoxia (1% O<sub>2</sub>) had no influence on EV production compared to hypoxia exposure alone (1% O<sub>2</sub>:  
264 1673 ± 60 EVs/cell vs 1% O<sub>2</sub> DFO: 1733 ± 87 EVs/cell, *p* > 0.05) (Figure 3A). Chemically induced  
265 hypoxia by desferrioxamine was confirmed by Western blot detection of HIF-1α in cells incubated in  
266 normoxia. (Figure 3B).

267 **3.2 Viability and apoptosis**

268 Cells exposed to 1% O<sub>2</sub> had similar caspase 3/7 activity to control cells (688 ± 7 vs 612 ± 73, relative  
269 luminescence units (RLU) *p* > 0.05). No difference was found in cell viability for cells exposed to 1%  
270 O<sub>2</sub> compared to control cells assessed either by the MTS cell proliferation assay (1% O<sub>2</sub>: 1.99 ± 0.04  
271 vs normoxia: 1.73 ± 0.24, absorbance [AU], *p* > 0.05), or by trypan blue exclusion (1% O<sub>2</sub>: 87 ± 1%  
272 vs normoxia: 89 ± 1%, *p* > 0.05)

273

### 274 **3.3 Morphology of HECV and HECV-derived-EVs.**

275 Scanning electron microscopy confirmed the release of EVs from HECVs. Cells were homogenous  
276 and approximately 10-15  $\mu\text{m}$  in diameter. Appendix Figure A4A shows HECVs incubated in  
277 normoxic (21%  $\text{O}_2$ ) conditions. Cells appear relatively dormant and have distinct cell boundaries.  
278 Appendix Figure A4B shows HECV cells incubated in hypoxic conditions (1%  $\text{O}_2$ ) for 24 hours.  
279 These cells appear rounded, producing a higher number of vesicles compared to the normoxic cells.  
280 Transmission electron microscopy confirmed the presence of EVs isolated from HECVs incubated in  
281 normoxia (Appendix Figure A4C) and hypoxia (Appendix Figure A4D). These EVs appear granular  
282 and approximately 100-250 nm in diameter.

### 283 **3.4 Characterisation of EVs**

284 Flow cytometry confirmed the presence of VCAM-1, ICAM-1, PECAM-1, P-selectin and E-selectin  
285 on HECVs which did not alter after hypoxia exposure ( $p > 0.05$ , Appendix Figure A5A). The  
286 presence of these adhesion molecules was reflected in the EVs. However these also did not change as  
287 a function of hypoxia exposure ( $p > 0.05$ , Appendix Figure A5B). There were no differences in the  
288 proportion of annexin V positive EVs between hypoxia-derived EVs ( $11 \pm 0.2\%$ ) and normoxia-  
289 derived EVs ( $11 \pm 0.25\%$ ,  $p > 0.05$ ).

290 Time-resolved fluorescence revealed no difference between the level of the exosomal markers CD9,  
291 TSG101 or ALIX and the endothelial marker VE-Cadherin in EVs isolated from normoxia and  
292 hypoxia (CD9: 21%  $\text{O}_2$ ;  $37651 \pm 1724$  vs 1%  $\text{O}_2$ ;  $39528 \pm 2507$ . TSG101: 21%  $\text{O}_2$ ;  $14495 \pm 549$  vs  
293 1%  $\text{O}_2$ ;  $15979 \pm 1953$ . ALIX: 21%  $\text{O}_2$ ;  $8683 \pm 818$  vs 1%  $\text{O}_2$ ;  $10310 \pm 510$ . CD144: 21%  $\text{O}_2$ ;  $2182 \pm$   
294  $178$  vs 1%  $\text{O}_2$ ;  $2601 \pm 234$ , arbitrary units,  $p > 0.05$ ) (Figure 2). HIF-1 $\alpha$  was present in EVs isolated  
295 from hypoxic HECVs and absent in those isolated from normoxia (21%  $\text{O}_2$ ;  $115 \pm 25$  vs 1%  $\text{O}_2$ ;  
296  $10310 \pm 520$ ,  $p < 0.001$ ) (Appendix Figure A6).

### 297 **3.5 Effect of silencing HIF-1 $\alpha$ and HIF-2 $\alpha$**

298 To confirm the role of HIF-1 $\alpha$  and/or HIF-2 $\alpha$  in the hypoxic enhancement of EV release, HECVs  
299 were transfected with a siRNA targeting either HIF-1 $\alpha$ , or HIF-2 $\alpha$ . Cells transfected with HIF-1 $\alpha$   
300 siRNA failed to show an enhancement in EV release following hypoxia compared to cells transfected  
301 with control siRNA or cells exposed to hypoxia alone (HIF-1 $\alpha$  siRNA in 1%  $\text{O}_2$ :  $243 \pm 20$  EVs/cell,  
302 control siRNA in 1%  $\text{O}_2$ :  $1680 \pm 473$  EVs/cell, 1%  $\text{O}_2$ :  $1680 \pm 250$  EVs/cell,  $p < 0.001$ ) (Figure 4A).  
303 EV production in cells transfected with HIF-1 $\alpha$  siRNA in hypoxia was similar to that of the normoxia  
304 control ( $158 \pm 38$  EVs/cell,  $p > 0.05$ ). HECVs were also transfected with HIF-2 $\alpha$  siRNA. Unlike HIF-  
305 1 $\alpha$  siRNA transfection, HIF-2 $\alpha$  silencing had no effect on EV production compared to cells  
306 transfected with control siRNA or exposed to hypoxia alone (HIF-2 $\alpha$  siRNA in 1%  $\text{O}_2$ :  $1549 \pm 46$   
307 EVs/cell, control siRNA in 1%  $\text{O}_2$ :  $1608 \pm 69$  EVs/cell, 1%  $\text{O}_2$ :  $1774 \pm 132$  EVs/cell,  $p < 0.05$ ).

308 Western blotting confirmed that cells transfected with HIF-1 $\alpha$  and HIF-2 $\alpha$  siRNA successfully  
309 inhibited gene expression, whilst the control siRNA had no impact on HIF-1 $\alpha$ /2 $\alpha$  expression (Figure  
310 4C, 4D).

### 311 **3.6 Effect of sodium nitrite on EV production**

312 To assess the effect of NO on the hypoxia-mediated enhancement of EV production, HECVs were  
313 treated with NaNO<sub>2</sub>. There was little evidence to suggest that NaNO<sub>2</sub> had any effect on EV production  
314 at 21% O<sub>2</sub>, (21% O<sub>2</sub>: 132  $\pm$  15 EVs/cell vs 21% O<sub>2</sub> + NaNO<sub>2</sub>: 125  $\pm$  19 EVs/cell,  $p > 0.05$ ). However,  
315 NaNO<sub>2</sub> significantly reduced the hypoxic enhancement of EV production (1% O<sub>2</sub>: 1859  $\pm$  67 EVs/cell  
316 vs. 1% O<sub>2</sub> + NaNO<sub>2</sub>: 905  $\pm$  78 EVs/cell,  $p < 0.001$ ). Treatment of HECVs in hypoxia with allopurinol  
317 in addition to NaNO<sub>2</sub> attenuated the NaNO<sub>2</sub>-induced suppression of hypoxia-mediated EV release,  
318 (1% O<sub>2</sub> + NaNO<sub>2</sub>; 905  $\pm$  78 EVs/cell vs 1% O<sub>2</sub>, NaNO<sub>2</sub> + Allopurinol; 1414  $\pm$  141 EVs/cell,  $p$   
319  $< 0.001$ ). Allopurinol alone had no effect on EV production in hypoxia (1824  $\pm$  69 EVs/cell,  $p > 0.05$   
320 (Figure 4B). The NO donor S-Nitrosoglutathione (GSNO) also significantly reduced EV production in  
321 hypoxia (896  $\pm$  27 EVs/cell,  $p < 0.001$ ) (Figure 5A). Western blots confirmed that NaNO<sub>2</sub> addition in  
322 hypoxia reduced the expression of HIF-1 $\alpha$ . The addition of allopurinol in the presence of NaNO<sub>2</sub>  
323 appeared to restore HIF-1 $\alpha$  expression in HECVs (Figure 5B).

### 324 **3.7 Effect of hypoxia and sodium nitrite on EV production in HUVECs**

325 In order to validate our findings in the HECV cell line, the effect of hypoxia and sodium nitrite on EV  
326 production was also assessed in HUVECs. NaNO<sub>2</sub> had no effect on EV production in normoxia (21%  
327 O<sub>2</sub>: 43  $\pm$  5.6 EVs/cell vs 21% O<sub>2</sub> + NaNO<sub>2</sub>: 41  $\pm$  4 EVs/cell,  $p > 0.05$ ). Hypoxia greatly enhanced EV  
328 production compared to normoxia (1% O<sub>2</sub>: 291  $\pm$  23 EVs/cell vs 21% O<sub>2</sub>: 43  $\pm$  6 EVs/cell,  $p < 0.001$ ).  
329 Furthermore, the addition of NaNO<sub>2</sub> significantly reduced EV production in hypoxia (1% O<sub>2</sub> +  
330 NaNO<sub>2</sub>: 153  $\pm$  11 EVs/cell vs 1% O<sub>2</sub>: 291  $\pm$  23 EVs/cell,  $p < 0.001$ ) (Figure 6A). Western blots  
331 confirmed that NaNO<sub>2</sub> addition in hypoxia reduced the expression of HIF-1 $\alpha$  (Figure 6B).

#### 332 4. Discussion

333 Our study shows that hypoxia-induced enhancement in EV production is mediated by HIF-1 $\alpha$  in  
334 endothelial cells. We extend these observations to show that NO<sub>2</sub><sup>-</sup> alleviates EV production selectively  
335 during hypoxia at least in part by reduction to NO via xanthine oxidoreductase, in turn favouring the  
336 oxygen sensitive degradation of HIF-1 $\alpha$  and subsequent suppression of HIF-mediated EV release.

337 During pathological conditions cellular O<sub>2</sub> levels can often be insufficient to meet physiological  
338 demands. The resulting hypoxia is an important feature of cardiovascular disease, sleep apnoea, and  
339 cancer and is associated with poor patient outcomes [45]. Endothelial cells exposed to hypoxia for 24  
340 hours demonstrated enhanced EV production at 5% O<sub>2</sub> and lower. This is in accordance with previous  
341 studies which have demonstrated that hypoxia is associated with increased endothelial-derived EV  
342 production *in vivo* [16,17]. Arterial blood pO<sub>2</sub> is normally within the range 10-14% O<sub>2</sub> (75-100  
343 mmHg), with venous levels approximately 4-5.5% O<sub>2</sub> (30-40 mmHg). At an arterial O<sub>2</sub> of 8% (60  
344 mmHg) there is a steep decline in oxygen saturation, and a human would require supplemental  
345 breathing, whereas <4% O<sub>2</sub> (26 mmHg) can be considered extreme hypoxia [46]. Given these  
346 reference ranges, we rationalised 5% O<sub>2</sub> in our studies represents an accurate model of a hypoxic  
347 condition for cells in culture, whereas less than 1% O<sub>2</sub> reflects severe hypoxia.

348 Endothelial EV signalling has been shown to enhance activation and adhesion of platelets, leading to  
349 the formation of a thrombus [47]. Studies have shown that increased EV release by activated  
350 endothelial cells was associated with cardiovascular events in patients with stroke history [48]. It  
351 remains unclear whether the pathological effects of these vesicles are due to differences in biological  
352 cargo compared to vesicles released under resting conditions, or simply due to an increased number of  
353 vesicles being produced. In our studies, we failed to measure a difference in numerous adhesion  
354 molecules between vesicles released from cells in hypoxia compared to cells in normoxia.

355 Interestingly, we found HIF-1 $\alpha$  was present in our EV sample, and was elevated under hypoxic  
356 conditions, potentially allowing for paracrine signalling to nearby cells. Previous studies have shown  
357 that nuclear translocation is not required for HIF-1 $\alpha$  stabilization after its translation in the cytoplasm  
358 [49], and thus may be packaged into EV during their formation via the classical pathway of exosome  
359 formation. This pathway is governed by the endosomal sorting complex required for transport  
360 (ESCRT), which orchestrates the formation of intraluminal vesicles within multivesicular bodies  
361 following invagination of the cells plasma membrane [50]. Notably, we were unable to detect HIF-1 $\alpha$   
362 in EVs derived from HIF-1 $\alpha$  siRNA treated cells.

363 Consistent with previous reports in breast cancer cell lines [51] we provide evidence that HIF-1 $\alpha$  is  
364 pivotal in the hypoxia-induced enhancement of EV release in endothelial cells. In contrast, HIF-2 $\alpha$   
365 had no influence on hypoxic EV production. Thus, hypoxia-mediated EV production may utilise

366 common cellular pathways regardless of the cell type. HIF-1 $\alpha$  is thought to be involved in acute  
367 hypoxia (2-24 hours), with HIF-2 $\alpha$  involved in cellular adaptation to chronic hypoxia (>24 hours)  
368 [52,53]. A third HIF isoform, HIF-3 $\alpha$ , also regulates the cellular response to hypoxia but was not  
369 studied here. HIF-3 $\alpha$  lacks the transactivation domain found in both HIF-1 $\alpha$  and HIF-2 $\alpha$  isoforms, and  
370 is said to be a negative regulator of HIF-1 $\alpha$  and HIF-2 $\alpha$  induced gene expression [54].

371 Acute hypoxia has been shown to increase calcium to levels similar to those observed during agonist  
372 stimulation of endothelial cells, but too low to cause apoptosis or a reduction in viability [55]. The  
373 mechanism of EV release by cells is still not fully characterised, although it is known to be dependent  
374 on a rise in cytosolic calcium, and subsequent activation of calpain and protein kinases, allowing  
375 cytoskeletal remodelling, translocation of phosphatidylserine, and enhanced permeability to  
376 potassium with associated osmotic effects [56–60]. Indeed, HIF-1 $\alpha$  activation has recently been  
377 shown to permit cytoskeleton reorganization in endothelial cells [61]. Furthermore, RAB22A has  
378 previously been identified as a potential mediator of HIF-1 $\alpha$  induced EV release. RAB22A is a small  
379 GTPase involved in trafficking between endosomal compartments, which is localised to budding EVs  
380 [62]. A study by Wang *et al* showed expression of this GTPase was HIF-1 $\alpha$  mediated, with RAB22A  
381 knockdown completely eliminating the increase in EV production in hypoxia [63].

382 Moreover, HIF has previously been shown to induce autophagy, via upregulation of the BNIP-3 gene,  
383 promoting the BNIP-3/Beclin pathway [64]. Additionally, HIF-1 $\alpha$  is an inhibitor of the mammalian  
384 target of rapamycin (mTOR), via upregulation of the target genes REDD1 and REDD2 [65]. mTOR is  
385 a key regulator of autophagy induction, with activated mTOR suppressing autophagy, and negative  
386 regulation of mTOR promoting it [66]. Autophagy and exosome release are coordinated mechanisms  
387 that share common cellular machinery [67], with some studies showing that induction of autophagy  
388 enhances EV release [68]. Indeed, the p38 mitogen-activated protein kinase (MAPK) that is involved  
389 in autophagy has also been shown to enhance procoagulant endothelial EV release [56]. This pathway  
390 could therefore explain the increase in EV generation seen in this study.

391 To our knowledge this is the first study to demonstrate that NO alleviates the hypoxic enhancement of  
392 EV production in endothelial cells, through the hypoxia-selective reduction of NO<sub>2</sub><sup>-</sup> to NO via  
393 xanthine oxidoreductase. This reduction was observed in both an endothelial cell line (HECVs) and  
394 primary endothelial cells (HUVECs). This observation is supported by previous work which showed  
395 impaired NO production induces endothelial EV production *in vitro* [32]. In contrast to the  
396 constitutively expressed  $\beta$ -subunit of HIF, HIF-1 $\alpha$  is an oxygen-regulated subunit. Numerous factors  
397 have been shown to modulate HIF-1 $\alpha$  activation and stabilisation in general, including NO [69]. NO<sub>2</sub><sup>-</sup>  
398 represents a bioactive “storage pool” for NO under certain conditions, such as hypoxia. This pathway,  
399 dubbed the “nitrate-nitrite-nitric oxide pathway”, has been said to complement the L-arginine-eNOS



400 pathway perfectly, ensuring NO production continues during conditions where oxygen-dependent  
401 eNOS activity is compromised. Indeed we, and others, have previously shown that  $\text{NO}_2^-$  administered  
402 intravenously can protect against vascular reperfusion injury [70,71].

403 The regulation of HIF-1 $\alpha$  by NO in hypoxia involves the mitochondrial cytochrome c oxidase (CcO),  
404 which plays a central role in oxidative phosphorylation and ATP synthesis. NO can readily modulate  
405 the activity of CcO and therefore its  $\text{O}_2$  consumption. In hypoxia, competitive binding of NO inhibits  
406 CcO allowing the redistribution of intracellular  $\text{O}_2$ , leading to increased  $\text{O}_2$  availability for prolyl  
407 hydroxylation and subsequent degradation of HIF-1 $\alpha$ , which has been shown by numerous studies  
408 [30,31,69]. Collectively, our data suggest that although HIF-1 appears to be the master hypoxic  
409 regulator which governs hypoxia-induced EV release, under hypoxic conditions  $\text{NO}_2^-$  is metabolised  
410 to NO, promoting the degradation of HIF-1 $\alpha$  and subsequent suppression of EV release. Interestingly,  
411 HIF-1 $\alpha$  can enhance NO production via upregulation of inducible nitric oxide synthase (iNOS),  
412 highlighting a potential negative feedback mechanism [72,73].

413 Treatment of endothelial cells with allopurinol, in the presence of  $\text{NaNO}_2$ , largely inhibited the  $\text{NO}_2^-$ -  
414 attributed suppression of EV production. This confirms that under hypoxic conditions, xanthine  
415 oxidoreductase plays an important role in the reduction of  $\text{NO}_2^-$  to NO. However, the presence of  
416 allopurinol failed to completely restore EV production seen in hypoxia alone, and it is therefore likely  
417 that multiple mechanisms, including mitochondrial reduction and aldehyde dehydrogenase play a role  
418 in reducing  $\text{NO}_2^-$  to NO in endothelial cells [74].

419 In summary, this study suggests a novel means by which inorganic nitrite ( $\text{NO}_2^-$ ) alleviates the  
420 hypoxic enhancement in EV production. Future studies should further elucidate which downstream  
421 targets of HIF-1 $\alpha$  may be responsible for the increase in EV production, and investigate whether  
422 enhancing NO bioavailability affects EV levels in clinical models of ischaemia.

423 **Acknowledgements**

424 The authors would like to thank Dr Christopher Von Ruhland for his assistance with the electron  
425 microscopy.

426 **Sources of Funding**

427 This work was funded by a Health and Care Research Wales Scholarship (N.B.H), the Mrs. John  
428 Nixon Scholarship (G.R.W) and the Cardiac Research Development Fund (G.R.W).

429 **References**

- 430 [1] E. van der Pol, A.N. Böing, P. Harrison, A. Sturk, R. Nieuwland, Classification, functions, and  
 431 clinical relevance of extracellular vesicles., *Pharmacol. Rev.* 64 (2012) 676–705.  
 432 doi:10.1124/pr.112.005983.
- 433 [2] B. György, T.G. Szabó, M. Pásztói, Z. Pál, P. Misják, B. Aradi, et al., Membrane vesicles,  
 434 current state-of-the-art: Emerging role of extracellular vesicles, *Cell. Mol. Life Sci.* 68 (2011)  
 435 2667–2688. doi:10.1007/s00018-011-0689-3.
- 436 [3] M.E. Tushuizen, M. Diamant, A. Sturk, R. Nieuwland, Cell-derived microparticles in the  
 437 pathogenesis of cardiovascular disease: friend or foe?, *Arterioscler. Thromb. Vasc. Biol.* 31  
 438 (2011) 4–9. doi:10.1161/ATVBAHA.109.200998.
- 439 [4] F. Wendler, R. Favicchio, T. Simon, C. Alifrangis, J. Stebbing, G. Giamas, Extracellular  
 440 vesicles swarm the cancer microenvironment: from tumor–stroma communication to drug  
 441 intervention, *Oncogene.* (2016). doi:10.1038/onc.2016.253.
- 442 [5] C. D’Souza-Schorey, J.W. Clancy, Tumor-derived microvesicles: shedding light on novel  
 443 microenvironment modulators and prospective cancer biomarkers., *Genes Dev.* 26 (2012)  
 444 1287–99. doi:10.1101/gad.192351.112.
- 445 [6] N. Yamada, Y. Kuranaga, M. Kumazaki, H. Shinohara, K. Taniguchi, Y. Akao, et al.,  
 446 Colorectal cancer cell-derived extracellular vesicles induce phenotypic alteration of T cells  
 447 into tumor-growth supporting cells with transforming growth factor- $\beta$ 1-mediated suppression,  
 448 *Oncotarget.* 7 (2016) 27033–27043.
- 449 [7] S.A. Bellingham, B.B. Guo, B.M. Coleman, A.F. Hill, Exosomes: Vehicles for the Transfer of  
 450 Toxic Proteins Associated with Neurodegenerative Diseases?, *Front. Physiol.* 3 (2012) 124.  
 451 doi:10.3389/fphys.2012.00124.
- 452 [8] A. Schneider, M. Simons, Exosomes: vesicular carriers for intercellular communication in  
 453 neurodegenerative disorders, *Cell Tissue Res.* 352 (2013) 33–47. doi:10.1007/s00441-012-  
 454 1428-2.
- 455 [9] L.J. Vella, R.A. Sharples, R.M. Nisbet, R. Cappai, A.F. Hill, The role of exosomes in the  
 456 processing of proteins associated with neurodegenerative diseases, *Eur. Biophys. J.* 37 (2008)  
 457 323–332. doi:10.1007/s00249-007-0246-z.
- 458 [10] A.G. Thompson, E. Gray, S.M. Heman-Ackah, I. Mäger, K. Talbot, S. El Andaloussi, et al.,  
 459 Extracellular vesicles in neurodegenerative disease - pathogenesis to biomarkers., *Nat. Rev.*  
 460 *Neurol.* 12 (2016) 346–57. doi:10.1038/nrneurol.2016.68.
- 461 [11] L.L. Horstman, W. Jy, J.J. Jimenez, Y.S. Ahn, Endothelial microparticles as markers of  
 462 endothelial dysfunction., *Front. Biosci.* 9 (2004) 1118–35.
- 463 [12] A. Gaceb, M.C. Martinez, R. Andriantsitohaina, Extracellular vesicles: new players in  
 464 cardiovascular diseases., *Int. J. Biochem. Cell Biol.* 50 (2014) 24–8.  
 465 doi:10.1016/j.biocel.2014.01.018.
- 466 [13] M.J. Vanwijk, E. Vanbavel, a Sturk, R. Nieuwland, M icroparticles in cardiovascular diseases,  
 467 *Cardiovasc. Res.* 59 (2003) 277–287.
- 468 [14] P.-E. Rautou, A.-C. Vion, N. Amabile, G. Chironi, A. Simon, A. Tedgui, et al., Microparticles,  
 469 vascular function, and atherothrombosis., *Circ. Res.* 109 (2011) 593–606.  
 470 doi:10.1161/CIRCRESAHA.110.233163.
- 471 [15] C.M. Boulanger, A. Scoazec, T. Ebrahimian, P. Henry, E. Mathieu, A. Tedgui, et al.,  
 472 Circulating microparticles from patients with myocardial infarction cause endothelial  
 473 dysfunction., *Circulation.* 104 (2001) 2649–2652. doi:10.1161/hc4701.100516.
- 474 [16] R. V Vince, B. Christmas, A.W. Midgley, L.R. McNaughton, L.A. Madden, Hypoxia mediated  
 475 release of endothelial microparticles and increased association of S100A12 with circulating

- 476 neutrophils., *Oxid. Med. Cell. Longev.* 2 (2009) 2–6.
- 477 [17] M. Lichtenauer, B. Goebel, M. Fritzenwanger, M. Förster, S. Betge, A. Lauten, et al.,  
 478 Simulated temporary hypoxia triggers the release of CD31+/Annexin+ endothelial  
 479 microparticles: A prospective pilot study in humans., *Clin. Hemorheol. Microcirc.* (2014).  
 480 doi:10.3233/CH-141908.
- 481 [18] P. Vaupel, A. Mayer, Hypoxia in cancer: significance and impact on clinical outcome., *Cancer*  
 482 *Metastasis Rev.* 26 (2007) 225–39. doi:10.1007/s10555-007-9055-1.
- 483 [19] C. Peers, M.L. Dallas, H.E. Boycott, J.L. Scragg, H.A. Pearson, J.P. Boyle, Hypoxia and  
 484 neurodegeneration., *Ann. N. Y. Acad. Sci.* 1177 (2009) 169–77. doi:10.1111/j.1749-  
 485 6632.2009.05026.x.
- 486 [20] G.L. Semenza, Hypoxia-inducible factor 1: oxygen homeostasis and disease pathophysiology.,  
 487 *Trends Mol. Med.* 7 (2001) 345–50.
- 488 [21] O.G. de Jong, M.C. Verhaar, Y. Chen, P. Vader, H. Gremmels, G. Posthuma, et al., Cellular  
 489 stress conditions are reflected in the protein and RNA content of endothelial cell-derived  
 490 exosomes., *J. Extracell. Vesicles.* 1 (2012). doi:10.3402/jev.v1i0.18396.
- 491 [22] G.L. Semenza, HIF-1 mediates metabolic responses to intratumoral hypoxia and oncogenic  
 492 mutations., *J. Clin. Invest.* 123 (2013) 3664–71. doi:10.1172/JCI67230.
- 493 [23] C.M. Lambert, M. Roy, G.A. Robitaille, D.E. Richard, S. Bonnet, HIF-1 inhibition decreases  
 494 systemic vascular remodelling diseases by promoting apoptosis through a hexokinase 2-  
 495 dependent mechanism., *Cardiovasc. Res.* 88 (2010) 196–204. doi:10.1093/cvr/cvq152.
- 496 [24] H. Tian, S.L. McKnight, D.W. Russell, Endothelial PAS domain protein 1 (EPAS1), a  
 497 transcription factor selectively expressed in endothelial cells., *Genes Dev.* 11 (1997) 72–82.
- 498 [25] I.P. Stolze, D.R. Mole, P.J. Ratcliffe, Regulation of HIF: prolyl hydroxylases., *Novartis Found.*  
 499 *Symp.* 272 (2006) 15-25-36.
- 500 [26] C.P. Bracken, A.O. Fedele, S. Linke, W. Balrak, K. Lisy, M.L. Whitelaw, et al., Cell-specific  
 501 Regulation of Hypoxia-inducible Factor (HIF)-1 $\alpha$  and HIF-2 $\alpha$  Stabilization and  
 502 Transactivation in a Graded Oxygen Environment \*, (2006). doi:10.1074/jbc.M600288200.
- 503 [27] L. Østergaard, U. Simonsen, Y. Eskildsen-Helmond, H. Vorum, N. Uldbjerg, B. Honoré, et al.,  
 504 Proteomics reveals lowering oxygen alters cytoskeletal and endoplasmatic stress proteins in  
 505 human endothelial cells, *Proteomics.* 9 (2009) 4457–4467. doi:10.1002/pmic.200800130.
- 506 [28] L.E. Campbell, J. Nelson, E. Gibbons, A.M. Judd, J.D. Bell, Membrane Properties Involved in  
 507 Calcium-Stimulated Microparticle Release from the Plasma Membranes of S49 Lymphoma  
 508 Cells, *Sci. World J.* 2014 (2014) 1–7. doi:10.1155/2014/537192.
- 509 [29] K.M. Naseem, The role of nitric oxide in cardiovascular diseases., *Mol. Aspects Med.* 26  
 510 (2005) 33–65. doi:10.1016/j.mam.2004.09.003.
- 511 [30] T. Hagen, C.T. Taylor, F. Lam, S. Moncada, Redistribution of intracellular oxygen in hypoxia  
 512 by nitric oxide: effect on HIF1 $\alpha$ ., *Science.* 302 (2003) 1975–8.  
 513 doi:10.1126/science.1088805.
- 514 [31] E. Metzen, J. Zhou, W. Jelkmann, J. Fandrey, B. Brüne, Nitric oxide impairs normoxic  
 515 degradation of HIF-1 $\alpha$  by inhibition of prolyl hydroxylases., *Mol. Biol. Cell.* 14 (2003)  
 516 3470–81. doi:10.1091/mbc.E02-12-0791.
- 517 [32] J.-M. Wang, Y. Wang, J.-Y. Huang, Z. Yang, L. Chen, L.-C. Wang, et al., C-Reactive protein-  
 518 induced endothelial microparticle generation in HUVECs is related to BH4-dependent NO  
 519 formation., *J. Vasc. Res.* 44 (2007) 241–8. doi:10.1159/000100558.
- 520 [33] J.O. Lundberg, E. Weitzberg, M.T. Gladwin, The nitrate-nitrite-nitric oxide pathway in  
 521 physiology and therapeutics., *Nat. Rev. Drug Discov.* 7 (2008) 156–67. doi:10.1038/nrd2466.
- 522 [34] P.E. James, G.R. Willis, J.D. Allen, P.G. Winyard, A.M. Jones, Nitrate pharmacokinetics:

- 523 Taking note of the difference., *Nitric Oxide*. 48 (2015) 44–50. doi:10.1016/j.niox.2015.04.006.
- 524 [35] R.S. Khambata, S.M. Ghosh, A. Ahluwalia, “Repurposing” of Xanthine Oxidoreductase as a  
525 Nitrite Reductase: A New Paradigm for Therapeutic Targeting in Hypertension., *Antioxid.*  
526 *Redox Signal*. 23 (2015) 340–53. doi:10.1089/ars.2015.6254.
- 527 [36] H. Li, A. Samouilov, X. Liu, J.L. Zweier, Characterization of the magnitude and kinetics of  
528 xanthine oxidase-catalyzed nitrate reduction: evaluation of its role in nitrite and nitric oxide  
529 generation in anoxic tissues., *Biochemistry*. 42 (2003) 1150–9. doi:10.1021/bi026385a.
- 530 [37] K. Cosby, K.S. Partovi, J.H. Crawford, R.P. Patel, C.D. Reiter, S. Martyr, et al., Nitrite  
531 reduction to nitric oxide by deoxyhemoglobin vasodilates the human circulation., *Nat. Med.* 9  
532 (2003) 1498–505. doi:10.1038/nm954.
- 533 [38] S. Shiva, Z. Huang, R. Grubina, J. Sun, L.A. Ringwood, P.H. MacArthur, et al.,  
534 Deoxymyoglobin is a nitrite reductase that generates nitric oxide and regulates mitochondrial  
535 respiration, *Circ. Res.* 100 (2007) 654–661. doi:10.1161/01.RES.0000260171.52224.6b.
- 536 [39] S. Basu, N.A. Azarova, M.D. Font, S.B. King, N. Hogg, M.T. Gladwin, et al., Nitrite reductase  
537 activity of cytochrome c., *J. Biol. Chem.* 283 (2008) 32590–7. doi:10.1074/jbc.M806934200.
- 538 [40] P.R. Castello, P.S. David, T. McClure, Z. Crook, R.O. Poyton, Mitochondrial cytochrome  
539 oxidase produces nitric oxide under hypoxic conditions: implications for oxygen sensing and  
540 hypoxic signaling in eukaryotes., *Cell Metab.* 3 (2006) 277–87.  
541 doi:10.1016/j.cmet.2006.02.011.
- 542 [41] B. Baudin, A. Bruneel, N. Bosselut, M. Vaubourdolle, A protocol for isolation and culture of  
543 human umbilical vein endothelial cells., *Nat. Protoc.* 2 (2007) 481–5.  
544 doi:10.1038/nprot.2007.54.
- 545 [42] J. Webber, A. Clayton, How pure are your vesicles?, *J. Extracell. Vesicles*. 2 (2013).
- 546 [43] G.R. Willis, K. Connolly, K. Ladell, T.S. Davies, I.A. Guschina, D. Ramji, et al., Young  
547 women with polycystic ovary syndrome have raised levels of circulating annexin V-positive  
548 platelet microparticles., *Hum. Reprod.* 29 (2014) 2756–63. doi:10.1093/humrep/deu281.
- 549 [44] K.D. Connolly, I.A. Guschina, V. Yeung, A. Clayton, M.S. Draman, C. Von Ruhland, et al.,  
550 Characterisation of adipocyte-derived extracellular vesicles released pre- and post-  
551 adipogenesis., *J. Extracell. Vesicles*. 4 (2015) 29159.
- 552 [45] G.L. Semenza, Oxygen sensing, hypoxia-inducible factors, and disease pathophysiology.,  
553 *Annu. Rev. Pathol.* 9 (2014) 47–71. doi:10.1146/annurev-pathol-012513-104720.
- 554 [46] J.-A. Collins, A. Rudenski, J. Gibson, L. Howard, R. O’Driscoll, Relating oxygen partial  
555 pressure, saturation and content: the haemoglobin-oxygen dissociation curve., *Breathe*  
556 (Sheffield, England). 11 (2015) 194–201. doi:10.1183/20734735.001415.
- 557 [47] P. Cherian, G.J. Hankey, J.W. Eikelboom, J. Thom, R.I. Baker, A. McQuillan, et al.,  
558 Endothelial and platelet activation in acute ischemic stroke and its etiological subtypes.,  
559 *Stroke*. 34 (2003) 2132–7. doi:10.1161/01.STR.0000086466.32421.F4.
- 560 [48] S.-T. Lee, K. Chu, K.-H. Jung, J.-M. Kim, H.-J. Moon, J.-J. Bahn, et al., Circulating CD62E+  
561 microparticles and cardiovascular outcomes., *PLoS One*. 7 (2012) e35713.  
562 doi:10.1371/journal.pone.0035713.
- 563 [49] E. Berra, D. Roux, D.E. Richard, J. Pouyssegur, Hypoxia-inducible factor-1 alpha (HIF-1  
564 alpha) escapes O(2)-driven proteasomal degradation irrespective of its subcellular localization:  
565 nucleus or cytoplasm., *EMBO Rep.* 2 (2001) 615–20. doi:10.1093/embo-reports/kve130.
- 566 [50] M. Colombo, G. Raposo, C. Théry, Biogenesis, Secretion, and Intercellular Interactions of  
567 Exosomes and Other Extracellular Vesicles, *Annu. Rev. Cell Dev. Biol.* 30 (2014) 255–289.  
568 doi:10.1146/annurev-cellbio-101512-122326.
- 569 [51] H.W. King, M.Z. Michael, J.M. Gleadle, Hypoxic enhancement of exosome release by breast

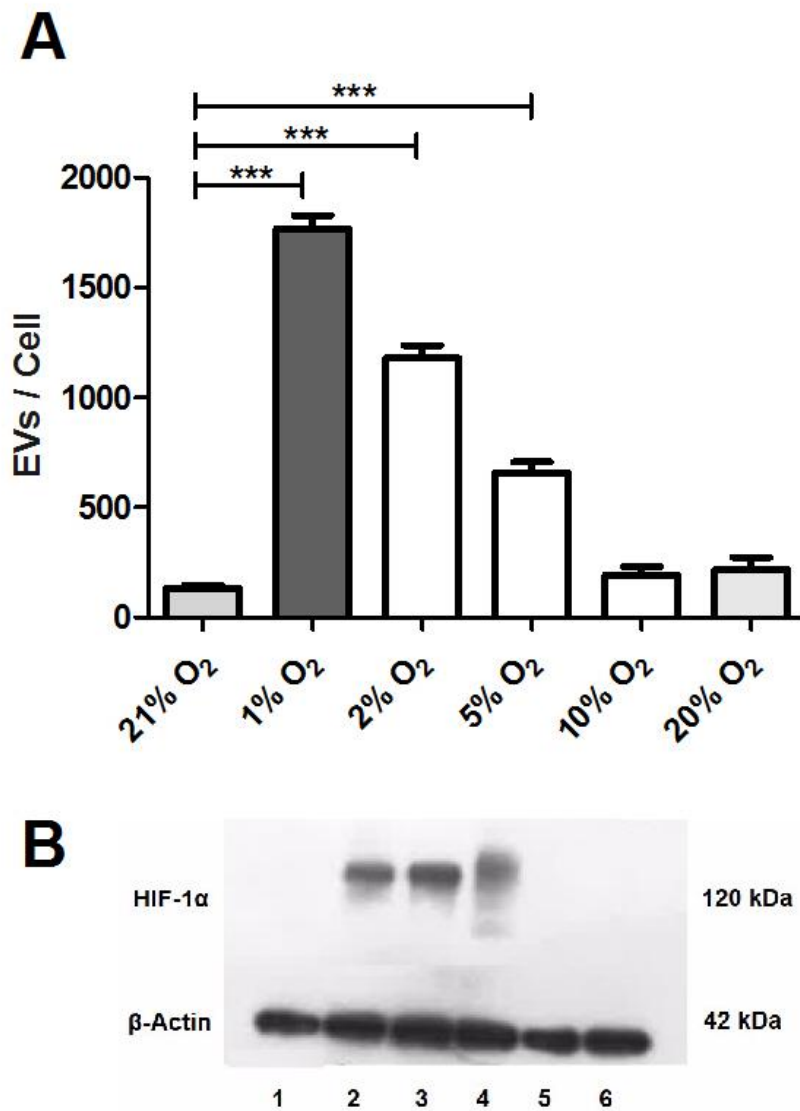
- 570 cancer cells., *BMC Cancer*. 12 (2012) 421. doi:10.1186/1471-2407-12-421.
- 571 [52] Q. Lin, X. Cong, Z. Yun, A. Harris, E. Rankin, A. Giaccia, et al., Differential hypoxic  
572 regulation of hypoxia-inducible factors 1alpha and 2alpha., *Mol. Cancer Res.* 9 (2011) 757–65.  
573 doi:10.1158/1541-7786.MCR-11-0053.
- 574 [53] M.Y. Koh, G. Powis, Passing the baton: the HIF switch., *Trends Biochem. Sci.* 37 (2012) 364–  
575 72. doi:10.1016/j.tibs.2012.06.004.
- 576 [54] P. Zhang, Q. Yao, L. Lu, Y. Li, P.-J. Chen, C. Duan, Hypoxia-inducible factor 3 is an oxygen-  
577 dependent transcription activator and regulates a distinct transcriptional response to hypoxia.,  
578 *Cell Rep.* 6 (2014) 1110–21. doi:10.1016/j.celrep.2014.02.011.
- 579 [55] T. Arnould, C. Michiels, I. Alexandre, J. Remacle, Effect of hypoxia upon intracellular  
580 calcium concentration of human endothelial cells., *J. Cell. Physiol.* 152 (1992) 215–21.  
581 doi:10.1002/jcp.1041520127.
- 582 [56] A.M. Curtis, P.F. Wilkinson, M. Gui, T.L. Gales, E. Hu, J.M. Edelberg, p38 mitogen-activated  
583 protein kinase targets the production of proinflammatory endothelial microparticles., *J.*  
584 *Thromb. Haemost.* 7 (2009) 701–9. doi:10.1111/j.1538-7836.2009.03304.x.
- 585 [57] S. Cauwenberghs, M.A.H. Feijge, A.G.S. Harper, S.O. Sage, J. Curvers, J.W.M. Heemskerk,  
586 Shedding of procoagulant microparticles from unstimulated platelets by integrin-mediated  
587 destabilization of actin cytoskeleton., *FEBS Lett.* 580 (2006) 5313–20.  
588 doi:10.1016/j.febslet.2006.08.082.
- 589 [58] P. Comfurius, J.M. Senden, R.H. Tilly, A.J. Schroit, E.M. Bevers, R.F. Zwaal, Loss of  
590 membrane phospholipid asymmetry in platelets and red cells may be associated with calcium-  
591 induced shedding of plasma membrane and inhibition of aminophospholipid translocase.,  
592 *Biochim. Biophys. Acta.* 1026 (1990) 153–60.
- 593 [59] E. Reichstein, A. Rothstein, Effects of quinine on Ca<sup>++</sup>-induced K<sup>+</sup> efflux from human red  
594 blood cells., *J. Membr. Biol.* 59 (1981) 57–63.
- 595 [60] D. Allan, P. Thomas, Ca<sup>2+</sup>-induced biochemical changes in human erythrocytes and their  
596 relation to microvesiculation., *Biochem. J.* 198 (1981) 433–40.
- 597 [61] A. Weidemann, J. Breyer, M. Rehm, K.-U. Eckardt, C. Daniel, I. Cicha, et al., HIF-1 $\alpha$   
598 activation results in actin cytoskeleton reorganization and modulation of Rac-1 signaling in  
599 endothelial cells, *Cell Commun. Signal.* 11 (2013) 80. doi:10.1186/1478-811X-11-80.
- 600 [62] J.G. Magadán, M.A. Barbieri, R. Mesa, P.D. Stahl, L.S. Mayorga, Rab22a regulates the sorting  
601 of transferrin to recycling endosomes., *Mol. Cell. Biol.* 26 (2006) 2595–614.  
602 doi:10.1128/MCB.26.7.2595-2614.2006.
- 603 [63] T. Wang, D.M. Gilkes, N. Takano, L. Xiang, W. Luo, C.J. Bishop, et al., Hypoxia-inducible  
604 factors and RAB22A mediate formation of microvesicles that stimulate breast cancer invasion  
605 and metastasis., *Proc. Natl. Acad. Sci. U. S. A.* 111 (2014) E3234-42.  
606 doi:10.1073/pnas.1410041111.
- 607 [64] G. Bellot, R. Garcia-Medina, P. Gounon, J. Chiche, D. Roux, J. Pouyssegur, et al., Hypoxia-  
608 induced autophagy is mediated through hypoxia-inducible factor induction of BNIP3 and  
609 BNIP3L via their BH3 domains., *Mol. Cell. Biol.* 29 (2009) 2570–81.  
610 doi:10.1128/MCB.00166-09.
- 611 [65] J. Brugarolas, K. Lei, R.L. Hurley, B.D. Manning, J.H. Reiling, E. Hafen, et al., Regulation of  
612 mTOR function in response to hypoxia by REDD1 and the TSC1/TSC2 tumor suppressor  
613 complex., *Genes Dev.* 18 (2004) 2893–904. doi:10.1101/gad.1256804.
- 614 [66] C.H. Jung, S.-H. Ro, J. Cao, N.M. Otto, D.-H. Kim, mTOR regulation of autophagy., *FEBS*  
615 *Lett.* 584 (2010) 1287–95. doi:10.1016/j.febslet.2010.01.017.
- 616 [67] F. Baixauli, C. L<sup>3</sup>pez-Ot<sup>3</sup>n, M. Mittelbrunn, Exosomes and Autophagy: Coordinated  
617 Mechanisms for the Maintenance of Cellular Fitness, *Front. Immunol.* 5 (2014) 403.

- 618 doi:10.3389/fimmu.2014.00403.
- 619 [68] C.M. Fader, D. Sánchez, M. Furlán, M.I. Colombo, Induction of autophagy promotes fusion of  
620 multivesicular bodies with autophagic vacuoles in k562 cells., *Traffic*. 9 (2008) 230–50.  
621 doi:10.1111/j.1600-0854.2007.00677.x.
- 622 [69] U. Berchner-Pfannschmidt, H. Yamac, B. Trinidad, J. Fandrey, Nitric oxide modulates oxygen  
623 sensing by hypoxia-inducible factor 1-dependent induction of prolyl hydroxylase 2., *J. Biol.*  
624 *Chem.* 282 (2007) 1788–96. doi:10.1074/jbc.M607065200.
- 625 [70] A. Webb, R. Bond, P. McLean, R. Uppal, N. Benjamin, A. Ahluwalia, Reduction of nitrite to  
626 nitric oxide during ischemia protects against myocardial ischemia-reperfusion damage, *Proc.*  
627 *Natl. Acad. Sci.* 101 (2004) 13683–13688. doi:10.1073/pnas.0402927101.
- 628 [71] T.E. Ingram, A.G. Fraser, R.A. Bleasdale, E.A. Ellins, A.D. Margulescu, J.P. Halcox, et al.,  
629 Low-dose sodium nitrite attenuates myocardial ischemia and vascular ischemia-reperfusion  
630 injury in human models., *J. Am. Coll. Cardiol.* 61 (2013) 2534–41.  
631 doi:10.1016/j.jacc.2013.03.050.
- 632 [72] F. Jung, L.A. Palmer, N. Zhou, R.A. Johns, Hypoxic regulation of inducible nitric oxide  
633 synthase via hypoxia inducible factor-1 in cardiac myocytes., *Circ. Res.* 86 (2000) 319–25.
- 634 [73] R. Hu, A. Dai, S. Tan, Hypoxia-inducible factor 1 alpha upregulates the expression of  
635 inducible nitric oxide synthase gene in pulmonary arteries of hypoxic rat., *Chin. Med. J.*  
636 (Engl). 115 (2002) 1833–7.
- 637 [74] S. Shiva, Nitrite: A Physiological Store of Nitric Oxide and Modulator of Mitochondrial  
638 Function., *Redox Biol.* 1 (2013) 40–44. doi:10.1016/j.redox.2012.11.005.
- 639

640 **Figures**

641 **Figure 1. The effect of hypoxia on EV concentration.** (A) EVs produced per cell at varying O<sub>2</sub>  
642 concentrations. (B) Western blot showing the presence and absence of HIF-1 $\alpha$  at varying O<sub>2</sub>  
643 concentrations. Lane 1: 21% O<sub>2</sub>. Lane 2: 1% O<sub>2</sub>. Lane 3: 2% O<sub>2</sub>. Lane 4: 5% O<sub>2</sub>. Lane 5: 10% O<sub>2</sub>. Lane  
644 6: 20% O<sub>2</sub>. Results represent [n = 5]. Each sample was analysed in quintuplicate and the mean was  
645 used in further analysis. Data are expressed as mean  $\pm$  SEM. \*\*\* reflects  $p < 0.001$ .

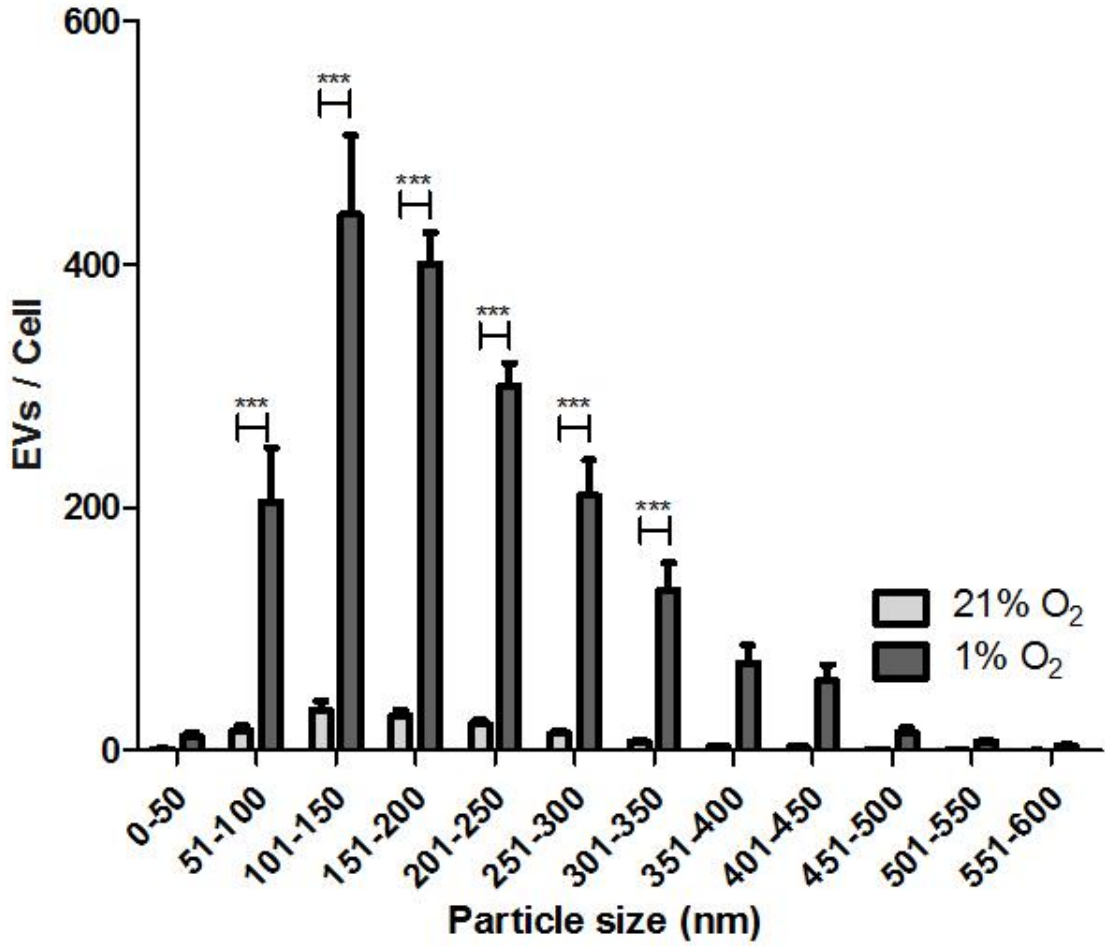
646



647



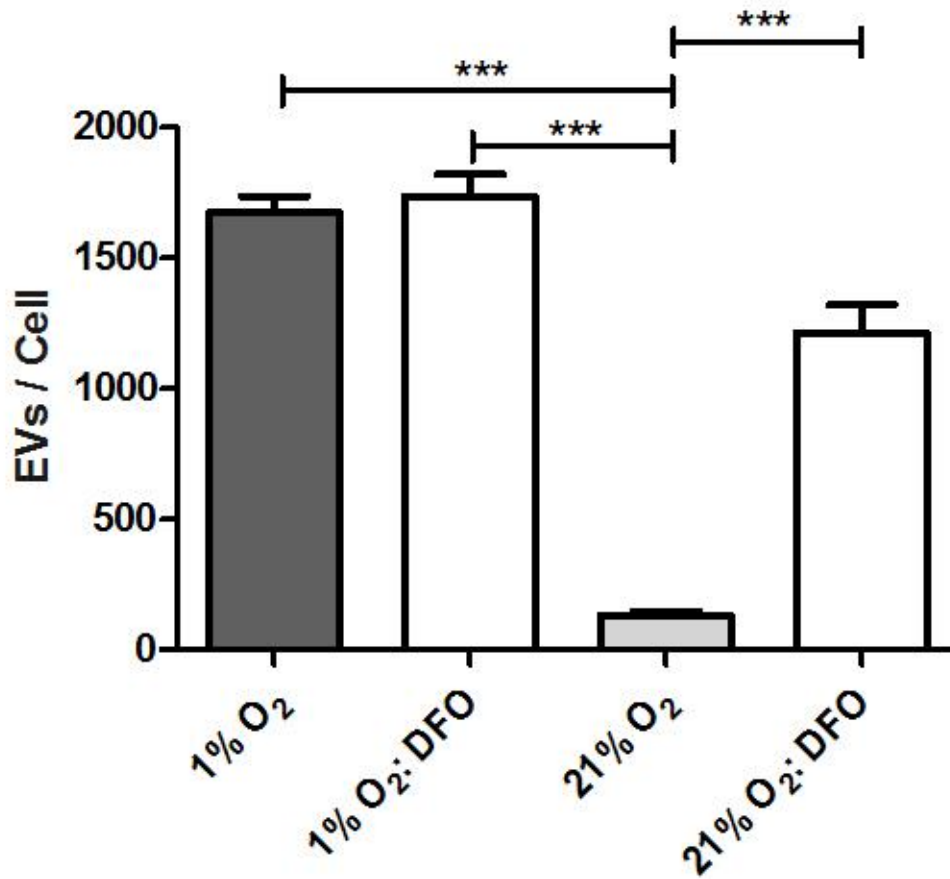
648 **Figure 2. The effect of hypoxia on EV size distribution.** Assessed in 50 nm bin sizes, results  
649 represent [n = 5]. Each sample was analysed in quintuplicate and the mean was used in further  
650 analysis. Data are expressed as mean  $\pm$  SEM. \*\*\* reflects  $p < 0.001$ .



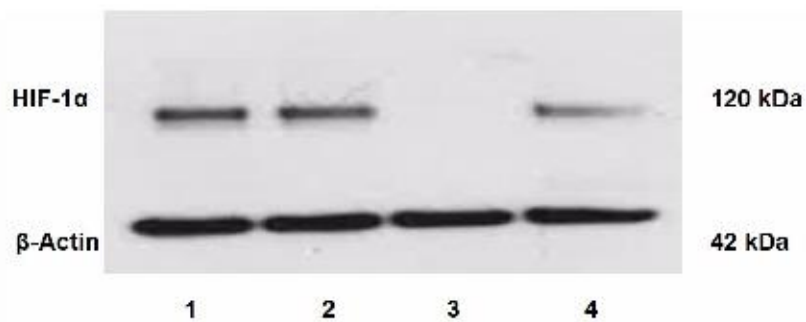
651

652 **Figure 3. The effect of the hypoxia mimetic agent desferrioxamine on EV production.** (A) EVs  
653 produced per cell. (B) Western blot confirming successful stabilisation of HIF-1 $\alpha$  in normoxia. Lane  
654 1: 1% O<sub>2</sub>. Lane 2: 1% O<sub>2</sub> + DFO. Lane 3: 21% O<sub>2</sub>. Lane 4: 21% O<sub>2</sub> + DFO. Results represent [N=5].  
655 Each sample was analysed in quintuplicate and the mean was used in further analysis. Data are  
656 expressed as mean  $\pm$  SEM. \*\*\* and \* reflect p < 0.001.

**A**

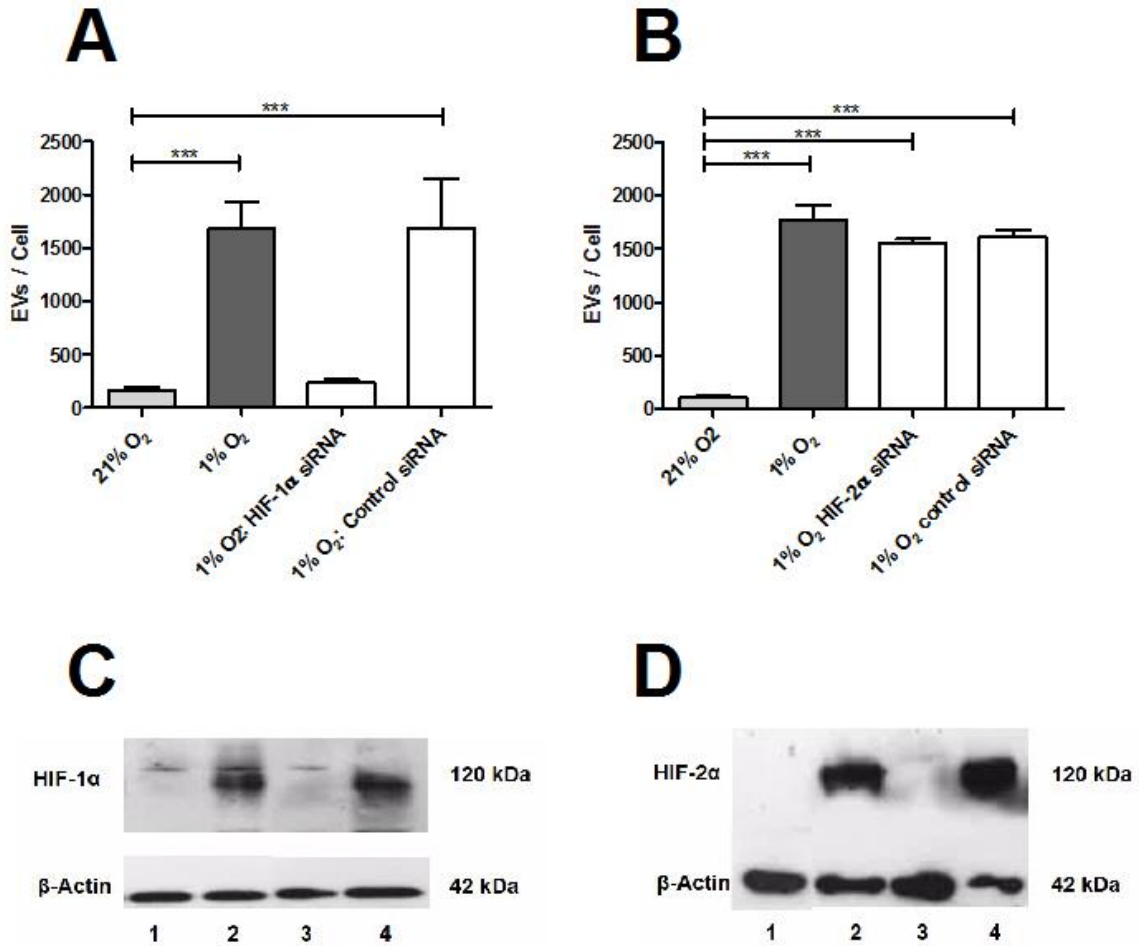


**B**



657

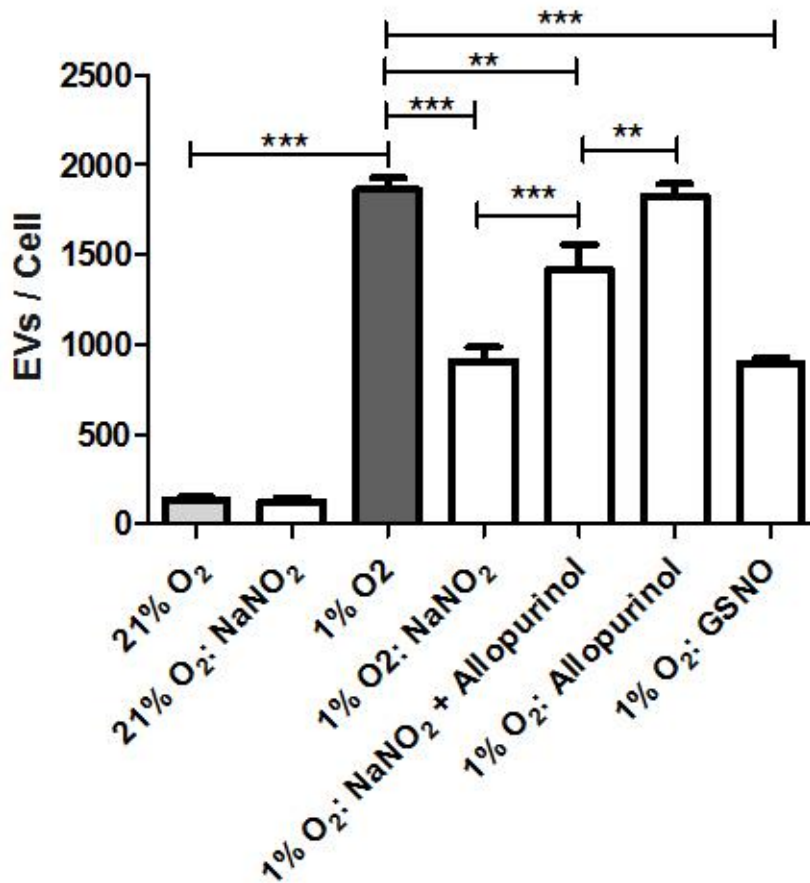
658 **Figure 4. The effect of silencing HIF-1 $\alpha$  and HIF-2 $\alpha$  on EV production.** (A) HIF-1 $\alpha$  siRNA; EVs  
 659 produced per cell. (B) HIF-2 $\alpha$  siRNA; EVs produced per cell. (C) Western blot confirming successful  
 660 silencing of HIF-1 $\alpha$ . Lane 1: 21% O<sub>2</sub>. Lane 2: 1% O<sub>2</sub>. Lane 3: 1% O<sub>2</sub>, HIF-1 $\alpha$  siRNA. Lane 4: 1% O<sub>2</sub>,  
 661 control siRNA. (D) Western blot confirming successful silencing of HIF-2 $\alpha$ . Lane 1: 21% O<sub>2</sub>. Lane 2:  
 662 1% O<sub>2</sub>. Lane 3: 1% O<sub>2</sub>, HIF-2 $\alpha$  siRNA. Lane 4: 1% O<sub>2</sub>, control siRNA. Results represent [*n* = 5]. Each  
 663 sample was analysed in quintuplicate and the mean was used in further analysis. Data are expressed as  
 664 mean  $\pm$  SEM. \*\*\* reflects *p* < 0.001.



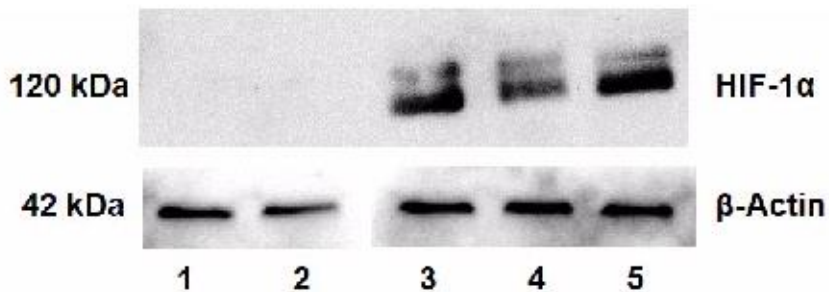
665

666 **Figure 5. The effect of sodium nitrite on EV production.** (A) EVs produced per cell following  
 667 exposure to various conditions. (B) Western blotting showing the expression of HIF-1 $\alpha$  under various  
 668 conditions. Lane 1: 21% O<sub>2</sub>. Lane 2: 21% O<sub>2</sub>, NaNO<sub>2</sub>. Lane 3: 1% O<sub>2</sub>. Lane 4: 1% O<sub>2</sub>, NaNO<sub>2</sub>. Lane 5:  
 669 1% O<sub>2</sub>, NaNO<sub>2</sub> and allopurinol. Results represent [*n* = 5]. Each sample was analysed in quintuplicate  
 670 and the mean was used in further analysis. Data are expressed as mean  $\pm$  SEM. \*\*, \*\*\* reflects *p* <  
 671 0.01, and *p* < 0.001 respectively.

**A**

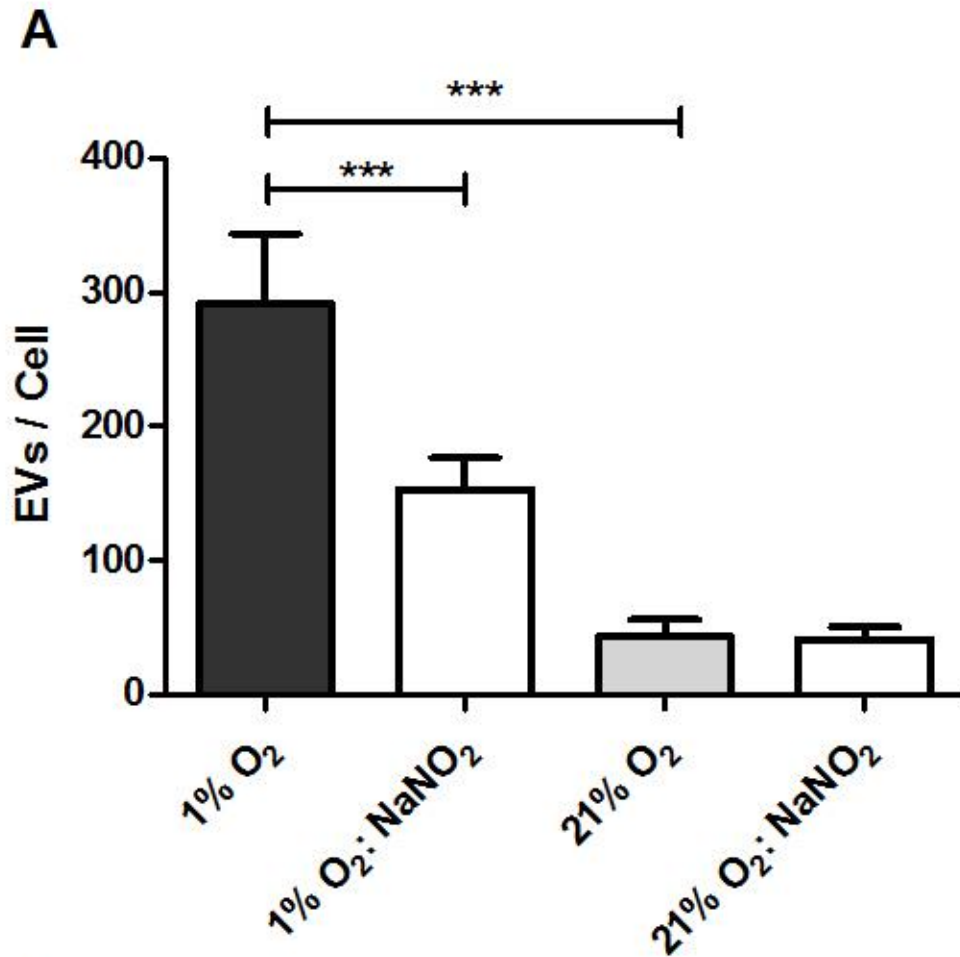


**B**



672

**Figure 6. The effect of hypoxia and sodium nitrite on EV production in HUVECs.** (A) EVs produced by HUVECs following exposure to hypoxia and/or NaNO<sub>2</sub>. (B) Western blotting showing the expression of HIF-1 $\alpha$  following exposure to hypoxia and/or NaNO<sub>2</sub>. Lane 1: 1% O<sub>2</sub>. Lane 2: 1% O<sub>2</sub> + NaNO<sub>2</sub>. Lane 3: 21% O<sub>2</sub>. Lane 4: 21% O<sub>2</sub> + NaNO<sub>2</sub>. Results represent [n=5]. Each sample was analysed in quintuplicate and the mean was used in further analysis. Data are expressed as mean  $\pm$  SEM. \*\*\* reflects  $p < 0.001$ .



**B**

